Speed Control for PMSM Servo System Using Predictive Functional Control and Extended State Observer

Huixian Liu and Shihua Li, *Senior Member, IEEE*

***Abstract*—The speed regulation problem for permanent magnet synchronous motor (PMSM) servo system is studied in this paper. In order to optimize the control performance of the PMSM servo system, the predictive functional control (PFC) method is introduced in the control design of speed loop. The PFC-based speed control design consists of two steps. A simplified model is employed to predict the future q-axis current of PMSM. Then, an optimal control law is obtained by minimizing a quadratic performance index. However, it is noted that the standard PFC method does not achieve a satisfying effect in the presence of strong disturbances. To this end, an improved PFC method, called the PFC+ESO method, is developed. It introduces extended state observer (ESO) to estimate the lumped disturbances and adds a feedforward compensation item based on the estimated disturbances to the PFC speed controller. Simulation and experiment comparisons are made for these PFC methods and proportional-integral method with antiwindup control method to verify the effectiveness of the proposed methods.**

***Index Terms*—Extended state observer (ESO), optimal control, permanent magnet synchronous motor (PMSM), predictive functional control (PFC).**

I. Introduction

PERMANENT magnet synchronous motor (PMSM) has gained a wide acceptance in motion control applications due to its high performance such as compact structure, high air-gap flux density, high power density, high torque to inertia ratio, and high efficiency [1]. Due to the existence of nonlinearities, uncertainties, and disturbances, conventional linear control methods, including the proportional-integral (PI) control method, cannot guarantee a sufficiently high performance for the PMSM servo system [2], [3]. To enhance the control performance, in recent years, many nonlinear control methods have been developed for the PMSM system, such as linearization control [4], adaptive control [5], [6], robust control [7], [8], sliding mode control [9], [10], disturbance observer-based control [6], [11]–[13], [34], finite time control [12], fractional order control [14], fuzzy control [2], [15], neural network control [3], [15], and so on. These approaches improve the control performance of the motor from different aspects.

Model predictive control (MPC) is one of the most practical advanced control technique in industrial applications [16]. It can be regarded as a kind of optimal control methods, which employs a dynamic model of plant to forecast the future behavior of states and determines the future control action according to optimization of a certain performance target function or an operating cost function at each sampling time [17], [18]. The MPC method can ensure a satisfying system performance since it possesses the advantages including robustness, simplicity of modeling, and good capability of handling constraints of both manipulated and controlled variables.

The well-known disadvantage of MPC method is that the calculation of control action requires a cumbersome computation load since it requires the solution of an optimization problem at each sampling time. The real-time requirement by the online optimization restricts the industrial applications of the MPC method to some extent during a long time. However, as the advanced development of computing hardware and the convex optimization technique, it is possible to implement these controllers for the fast-varying dynamical systems which have a high real-time requirement.

There are some such cheering research reports on the application of MPC method to the PMSM servo system [19]–[21]. An important reason for the growing application is its linear model can be obtained by both analytical means and identification techniques.

To enhance the tracking performance of d–q axis stator currents to the command currents, a MPC-based current controller is developed in [20] with simulation and experimental verification results. In [19], three kinds of predictive control methods for the current loop have been compared by theoretical analysis, simulation, and experimental verification results. In [21], the control structure which combines the speed and current control together, using only one single loop, is employed. The future control action is obtained by optimizing a cost function consisting of a future speed tracking error item and penalization items on the d–q axis stator currents as well as the manipulated variable, i.e., the d–q axis stator voltages.

The main purpose of this paper is to further advance the application of MPC in PMSM systems. There are possibly three contributions.

Manuscript received April 5, 2011; accepted June 30, 2011. Date of publication July 18, 2011; date of current version October 18, 2011. This work was supported by New Century Excellent Talents in University under Grant NCET-10-0328, National 863 Project of the Twelfth Five-Year Plan of China under Grant 2011AA04A106, National 863 Project of the Eleventh Five-Year Plan of China under Grant 2009AA04Z140, and Natural Science Foundation of Jiangsu Province under Project BK2008295.

The authors are with the Key Laboratory of Measurement and Control of CSE, School of Automation, Southeast University, Ministry of Education, Nanjing 210096, China (e-mail: lsh@seu.edu.cn).

Digital Object Identifier 10.1109/TIE.2011.2162217

First, a simplified MPC method, i.e., predictive functional control (PFC) method, is employed as the adopted control technique here. It is presented by Richalet [22]. While retaining the benefits of the MPC method such as online optimization and constraint handling, the PFC method produces an algorithm with a low online computation burden. It achieves computational simplicity by using simpler but more intuitive design guidelines. In the past decades, it has been successfully applied in industrial applications [23]–[27]. In [23], a PFC method is proposed for industrial robot. A predictive functional controller of quasi PI structure is developed in [25]. A fuzzy model-based predictive functional controller is proposed for the magnetic suspension system in [26]. In [27], an adaptive fuzzy model-based PFC scheme is introduced for a nonlinear, time-varying process. These results demonstrate that the PFC method exhibits remarkable robustness despite the model mismatch and uncontrolled dynamics.

Second, a different usage of MPC is considered. Note that the existing MPC results for PMSM systems either only consider the design for current loop [19], [20], or consider a control design for both speed and current variables without using the conventional cascade structure [21]. Since the control structure of cascade control loops is still a dominant control structure for the servo control problem, for the speed regulation problem here, the control scheme includes a speed loop and two current loops. The cascade architecture offers obvious advantages including the ability to resist disturbances and to improve set point response performance. Moreover, noting that the final control objective is to enhance the speed tracking performance other than the current tracking performance, we introduce the PFC method to the control design of speed loop. Compared with the cost function in [21], the cost function here is more simple, only requires a future speed tracking error item and a penalization item on the command q axis stator current.

Third, an improved PFC control method for the disturbance rejection ability of the PMSM system is developed. Note that in real industrial applications, PMSM systems always face with different disturbances, e.g., friction force, unmodeled dynamics, load disturbances. Note that the above PFC control method cannot achieve a satisfying effect in the presence of strong disturbances, which will be shown later in the simulation and experimental verification part. The reason is that MPC or PFC method does not handle the disturbances directly in its controller design procedure. Without any penalization item directly relative to disturbance rejection ability in the cost function, it is difficult to anticipate that the predictive controller reacts directly and promptly to reject disturbances, although they can asymptotically suppress disturbances through feedback regulation in a relatively slow way. This may cause a degradation of the closed-loop control performance in the presence of strong disturbances.

In this paper, to improve the disturbance rejection performance of the PFC control method, a feedforward compensation part for disturbances is introduced to the controller besides a PFC feedback part. Thus, a composite control scheme combining a feedforward compensation part based-extended state observer (ESO) and a feedback regulation part based on PFC, called PFC+ESO method, is developed. Since it is impossible to measure the disturbances, a kind of disturbance estimation technique is employed, i.e., ESO [28], [29]. It regards the lumped disturbances of the system, which consists of internal dynamics and external disturbances, as a new state of the system. This observer is one order more than the usual state observer. It can estimate both the states and the lumped disturbances. The ESO-based control schemes based on it (called active disturbance rejection control schemes) have been well studied and applied successively in many industrial control problems, e.g., robotic systems [30], machining processes [31], manipulator systems [32], power converter [33], PMSM systems [6], [34], other motor systems [35], [36] and general control systems [37], [38].

This paper is organized as follows. Section II introduces the PMSM drive model and the overview of PFC basics. Section III presents the design details of speed controller using the PFC method and the PFC+ESO method. The implementation, simulation, and experimental results of these predictive control schemes based on a discretized model of the PMSM in a full digital control system are also introduced in Section III. A conclusion is given in Section IV.

II. Preliminaries

This section describes the mathematical model of PMSM and the outline of the PFC method.

A. Mathematical Model of PMSM

Here, we consider a surface-mounted PMSM. Suppose that the three-phase stator windings of PMSM are sinusoidally distributed in space. For the purpose of control design, (i_d, i_q, ω) are chosen as state variables. The PMSM system can be written in the following explicit form [1]:

$$\begin{aligned}\frac{d\omega}{dt} &= \frac{K_t i_q}{J} - \frac{B\omega}{J} - \frac{T_L}{J}\\ \frac{di_d}{dt} &= -\frac{R_s i_d}{L_d} + n_p \omega i_q + \frac{u_d}{L_d}\\ \frac{di_q}{dt} &= -\frac{R_s i_q}{L_q} - n_p \omega i_d - \frac{n_p \phi_v \omega}{L_q} + \frac{u_q}{L_q}\end{aligned} \tag{1}$$

where L_d and L_q are the inductances of d–q axes satisfying $L_d = L_q = L$, u_d and u_q the stator voltages of d–q axes, i_d and i_q the stator currents of d–q axes, R_s the stator resistance, ω the rotor velocity, n_p the number of pole pairs, ϕ_d and ϕ_q the flux linkages of d–q axes, ϕ_v the rotor flux linkage, $K_t = 3n_p\phi_v/2$, T_L the load torque, J the moment of inertia, and B the viscous friction coefficient.

The general structure of the PMSM servo system investigated in this work is shown in Fig. 1. The overall system consists of a PMSM, a space vector pulse width modulation (SVPWM), a voltage-source inverter, a field-orientation mechanism, and three controllers. The controllers employ a structure of cascade control loops including a speed loop and two current loops. Here, two PI controllers are adopted in the two current loops

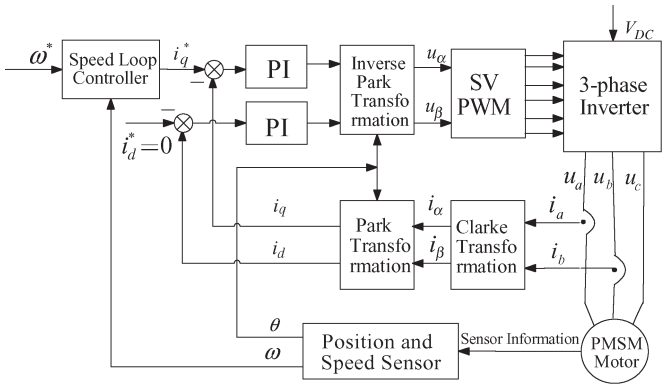

Fig. 1. Block diagram of the PMSM control system.

to stabilize the current tracking errors of d–q axes, respectively. As observed from Fig. 1, the rotor angular velocity ω (also the rotor position θ) can be obtained from the position and speed sensor. The currents i_d and i_q can be calculated from i_a and i_b (which can be obtained from measurements) by Clarke and Park transformations. Usually, the reference current i_d^* is set to be zero to maintain a constant flux operating condition. The reference current i_q^* is determined by the speed loop. The task here is to design a controller based on the PFC method for the speed loop.

B. Outline and Features of Predictive Functional Control Method

Compared with other predictive control methods, the PFC method can significantly reduce the volume of online computing, and make it possible and more suitable to be used in practical control of rapid dynamical system. As a type of MPC method, the main ideas of PFC can be summarized by the following points:

1) Base Functions: The future manipulated variables are structured as a linear prespecified combination of functions called base functions

$$u(k+i)=\sum_{j=1}^{N}\mu_j u_{bj}(i),\quad i=1,2,\ldots,P \tag{2}$$

where N the number of base functions, μ_j the coefficients to be computed during the optimization of the performance index, T_s the sample time, P the optimization horizon, $u_{bj}(i)$ the value of base function at time $t=iT_s$. The choice of these functions u_{bj} is determined by the form of reference signals. Generally, canonical functions are used, e.g., step, ramp, parabola, . . ., etc.

2) Prediction Model: A linear numerical model of the plant called internal model is used for online prediction of the future outputs over a defined finite horizon. In this instance, the prediction of the plant output is given by its model in discrete form

$$\begin{aligned} x_m(k)&=Ax_m(k-1)+Bu(k-1)\\ y_m(k)&=Cx_m(k)\quad (k=1,2,\ldots)\end{aligned} \tag{3}$$

where $x_m(k)$ is the state vector of prediction model, A, B, and C are the coefficient matrixes of state equation of the prediction model, respectively, and $y_m(k)$ is the output of the prediction model.

3) Error Correction: Considering the model mismatch, the impact of various kinds of interference and noise, there are some errors between forecasted model output and practical output. The prediction error is given by

$$e(k+P)=\ldots=e(k+1)=e(k)=y(k)-y_m(k). \tag{4}$$

where y is the measured system output.

4) Reference Trajectory: A reference trajectory provides a smooth transition toward the desired trajectory or set point within a certain future time horizon. The reference trajectory is given in the form of a reference model. The main goal of the proposed algorithm is to find a control law that enables the controlled signal to track the reference trajectory

$$y_r(k+i)=y^*(k+i)-\alpha_r^i\left[y^*(k)-y(k)\right],\quad i=1,2,\ldots,P \tag{5}$$

where y_r the reference trajectory, y^* the set value, $\alpha_r=e^{-(T_s/T_r)}$ the reference time constant, and T_r the desired response time of the closed-loop system.

5) Receding Optimization: The calculation of future control values is achieved by minimizing a sum of squared tracking errors plus a penalization on the control input. In this optimal index, the tracking error is between the predicted output and reference trajectory at some particular instants of the prediction horizon called coincidence points. The following cost function guarantees an optimal transition of the system output as closely as possible to the reference trajectory:

$$\begin{aligned} J_p=&\sum_{i=1}^{P}q_i^2\left[y_r(k+i)-y_m(k+i|k)-e(k+i)\right]^2\\ &+\sum_{j=1}^{M}r_j^2u^2(k+j-1)\end{aligned} \tag{6}$$

where M is the control horizon, parameter q_i allows an emphasis on each of the controlled outputs and its predictions, parameters r_j weighs the control efforts of inputs.

The general concept of the PFC method is shown in Fig. 2. Some industrial applications are constrained in order to ensure the safety of the process. Moreover, different elements of the process could be physically limited in their functioning. The aspect of these constraints can be added easily to the PFC algorithm by bounding the manipulated variable.

III. Design of Speed Controller

This section introduces the main design steps of the PFC method for the speed loop of PMSM.

A. Simplified Model of PMSM

MPC's popularity comes in great part from the fact that a suitable model can be obtained, thus the controller can be easily

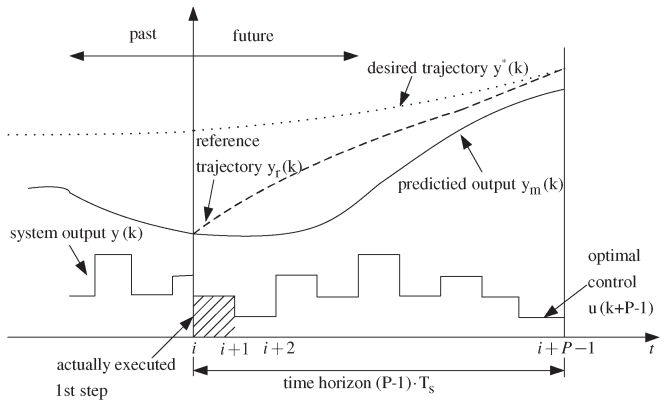

Fig. 2. General concept of the PFC method.

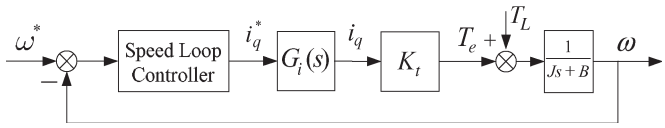

Fig. 3. Simplified control system block diagram.

implemented with a direct physically understandable model. It can be seen from (1) that the dynamic model of motor is nonlinear and state coupled since it contains product terms of motor speed ω with current i_d or i_q. In order to simplify the online implementation, a linear model is required. Since the dynamics of current loop is usually much faster than that of speed loop, it can be assumed to be ignored, which implies that the current i_q equals to the command current i_q^*, i.e., $G_i(s) \approx 1$. Thus, the diagram of PMSM can be reduced to the diagram shown in Fig. 3.

Now, the mechanical dynamics can be given in Laplace domain as a first-order model

$$\Omega(s) = \frac{K_t I_q^*(s) - T_L(s)}{Js + B}. \tag{7}$$

B. Design Based on Predictive Functional Control

1) Base Functions:

$$i_q^*(k+i) = \sum_{j=1}^{N} \mu_j u_{bj}(i), \quad i = 1, 2, \ldots, P. \tag{8}$$

Note that there is no restriction on the selection of these base functions, and the selection of base functions has no direct influence on the dynamics and stability of the closed-loop system [24]. The base function can be taken according to the form of the desired controlled variable. Here, we select the number of base functions as $N = 1$, this sequence is applied in a receding horizon fashion, that is

$$i_q^*(k) = \mu_1 \tag{9}$$

where $u_{bj}(i) = 1$, i.e., the base function is step response.

2) Prediction Model: As previously mentioned, PFC design requires a discrete time model. Here, a discrete time model, which is obtained by forward Euler discretization of (7), is given as follows:

$$\omega_m(k+1|k) = \alpha_m \omega_m(k) + K_m(1-\alpha_m) i_q^*(k) \tag{10}$$

where $\omega_m(k+1|k)$ is the prediction output of model at $(k+1)$th sampling time, i.e., $(k+1)T_s$, K_m and α_m are the coefficients of the differential equation of the prediction model.

Considering the prediction for time $(k+2)T_s$, we have

$$\omega_m(k+2|k) = \alpha_m \omega_m(k+1) + K_m(1-\alpha_m) i_q^*(k+1). \tag{11}$$

To obtain $\omega_m(k+2|k)$ at time kT_s, we have to replace $\omega_m(k+1)$ with $\omega_m(k+1|k)$, and assume that the future manipulated variables are a constant, i.e., $i_q^*(k) = i_q^*(k+1) = \cdots = i_q^*(k+P-1)$. This strategy is known as the mean-level control method. It means to consider a constant control input when predicting the system behavior, i.e., the control horizon $M = 1$ is chosen in (6) to obtain a simple but usually effective controller.

Thus, one can obtain

$$\omega_m(k+2|k) = \alpha_m^2 \omega_m(k) + K_m\left(1-\alpha_m^2\right) i_q^*(k). \tag{12}$$

In a similar way, the prediction output at time $(k+i)T_s$ is obtained as follows:

$$\omega_m(k+i|k) = \alpha_m^i \omega_m(k) + K_m\left(1-\alpha_m^i\right) i_q^*(k). \tag{13}$$

Then, the prediction output of (10) at times $k, k+1, \ldots, k+P$ can be rewritten in a matrix form

$$W_m(k) = W_o(k) + W_b(k)\mu_1(k) \tag{14}$$

where

$$W_m(k)_{(P\times 1)} = [\omega_m(k+1|k) \ \ldots \ \omega_m(k+P|k)]^T$$
$$W_o(k)_{(P\times 1)} = \left[\alpha_m \ \ldots \ \alpha_m^P\right]^T \omega_m(k)$$
$$W_b(k)_{(P\times 1)} = \left[K_m(1-\alpha_m) \ \ldots \ K_m\left(1-\alpha_m^P\right)\right]^T.$$

3) Error Correction:

$$e(k+P-1) = \ldots = e(k+1) = e(k) = \omega(k) - \omega_m(k) \tag{15}$$

where $\omega(k)$ is the actual output of system.

4) Reference Trajectory: A first-order exponential reference trajectory is used here

$$\omega_r(k+i) = \omega^*(k+i) - \alpha_r^i \left[\omega^*(k) - \omega(k)\right] \quad i = 1, 2, \ldots, P \tag{16}$$

where ω_r is for the reference trajectory, ω^* is the set point value.

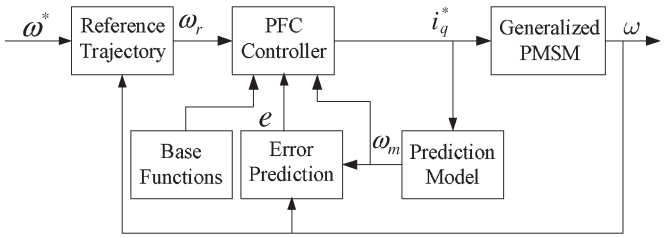

Fig. 4. Schematic diagram of the PMSM servo system using the PFC method.

5) Cost Function: The quadratic performance index of (6) is set as

$$\min J_p = \sum_{i=1}^{P} \left[\omega_r(k+i) - \omega_m(k+i) - e(k+i)\right]^2 + r^2 i_q^{*2}(k). \tag{17}$$

The cost function of (17) can be written as follows:

$$J_p = \left\|W_r(k) - W_m(k) - E(k)\right\|^2 Q + R i_q^{*2}. \tag{18}$$

where

$$\begin{aligned} \|X\|^2 A &= X^T A X; \\ W_r(k)_{(P\times 1)} &= \left[\omega_r(k+1) \ \ldots \ \omega_r(k+P)\right]^T \\ E(k)_{(P\times 1)} &= \left[e(k+1) \ \ldots \ e(k+P)\right]^T \\ Q_{(P\times P)} &= diag\left[q_1^2 \ \ldots \ q_P^2\right] \\ R_{(1\times 1)} &= r^2. \end{aligned}$$

Since the model (7) is linear, the minimal value of cost function (18) can be determined algebraically. The matrices W_b, W_r, W_o, and E must be updated at each sample time. Finally, by setting $\partial J/\partial i_q^{*2} = 0$, the controller is obtained as follows:

$$i_q^* = \left(W_b^T Q W_b + R\right)^{-1} W_b^T Q \left[W_r(k) - W_o(k) - E(k)\right]. \tag{19}$$

The block diagram of the PMSM system using the PFC method is shown in Fig. 4. Note that the "generalized PMSM" represents the two current loops which include PMSM and other components the same as that of Fig. 1.

C. Simulation and Experimental Results (PFC)

To demonstrate the efficiency of the proposed PFC method, simulations and experiments on a PMSM servo system have been performed. The PMSM system under two speed control schemes, i.e., PFC control and PI control, are compared by simulation and experimental results.

When using the standard PI algorithm for the speed controller for comparison here, it is very difficult to guarantee a good closed-loop performance in different work conditions, either large overshoots for fast responses or small overshoots but with slow responses. Therefore, an antiwindup PI algorithm [39] is employed here for the speed loop. Please note that when no confusion will arise, in the following descriptions, we simply refer such antiwindup PI controller as PI controller. The main idea of this antiwindup strategy can be described as follows:

$$\begin{aligned} e_1(k) &= \omega^*(k) - \omega(k) \\ if\ i_q^*(k-1) > I_{q\max}, \quad \alpha &= \begin{cases} 0, & e_1(k) > 0 \\ 1, & e_1(k) < 0 \end{cases} \\ if\ i_q^*(k-1) < -I_{q\max}, \quad \alpha &= \begin{cases} 0, & e_1(k) < 0 \\ 1, & e_1(k) > 0 \end{cases} \\ if\ -I_{q\max} \le i_q^*(k-1) \le I_{q\max}, \quad \alpha &= 1 \\ i_q^*(k) &= K_p * e_1(k) + K_i * \sum_{i=0}^{k} \alpha e_1(k). \end{aligned} \tag{20}$$

The parameters of a PMSM used in the simulation and experiment are given as: rated power $P = 750$ W, rated voltage $U = 200$ V, rated current $I_N = 4.71$ A, number of pole $n_p = 4$, armature resistance $R_s = 1.74\ \Omega$, stator inductances $L_d = L_q = L = 0.004$ H, viscous damping $B = 7.403 \times 10^{-5}$ N · m · s/rad, moment of inertia $J = 1.74 \times 10^{-4}$ Kg · m^2, rated speed $N = 3000$ rpm, rotor flux $\varphi_v = 0.1167$ wb, rated torque $T_N = 2.0$ N · m.

To have a fair comparison, first, let the control inputs of both algorithms have the same saturation limits. Second, by regulating the parameters of each control algorithm, let both closed-loop systems achieve relatively good performances.

1) Simulation Results: The parameters for PI speed controller are: $K_p = 0.11$, $K_i = 30$, for PFC speed controller are: the sample time $T_s = 250\ \mu$s, the desired response time $T_r = 50\ \mu$s, $P = 6$, $Q = I_{6\times 6}$, $r = 2$, $\alpha_m = 0.999$. The PI parameters of both current loops are the same: the proportional gains are 50, the integral gains are 2500. The saturation limit of i_q^* is ± 10 A.

Figs. 5 and 6 show that the PFC-based controller gives a shorter settling time with a smaller overshoot compared with the PI control method in the case of 2000 rpm reference speed. It can also be seen that, when a load torque $T_L = 2$ N · m is applied at $t = 0.5$ s and removed at $t = 0.6$ s, the standard PFC method has less speed fluctuations.

2) Experimental Results: To evaluate the performance of the proposed method, the experimental setup for a PMSM system has been built. The configuration of it and the experimental test setup are shown in Figs. 7 and 8, respectively.

The whole speed control algorithms including the SVPWM are implemented by the program of the DSP TMS320F2808 with a clock frequency of 100 MHZ. The control algorithm is implemented using C-program. The speed-loop and current-loop sampling periods are 250 μs and 60 μs, respectively. The saturation limit of i_q^* is ± 9.42 A. The PMSM is driven by a three-phase pulse width modulation (PWM) inverter with an intelligent power module with a switching frequency of 10 kHz. The phase currents are measured by the Hall-effect devices and are converted through two 12-bit analog to digital converters. An incremental position encoder of 2500 lines is used to measure the rotor speed and absolute rotor position.

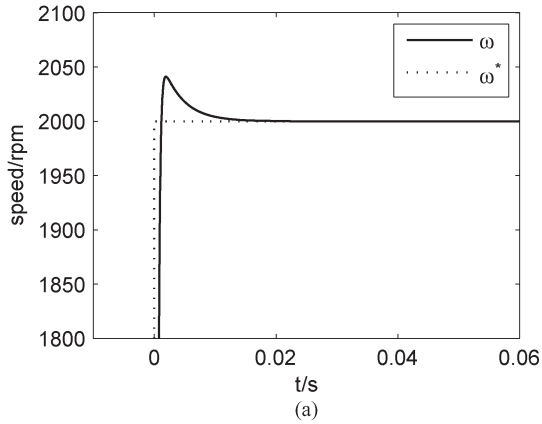

(a)

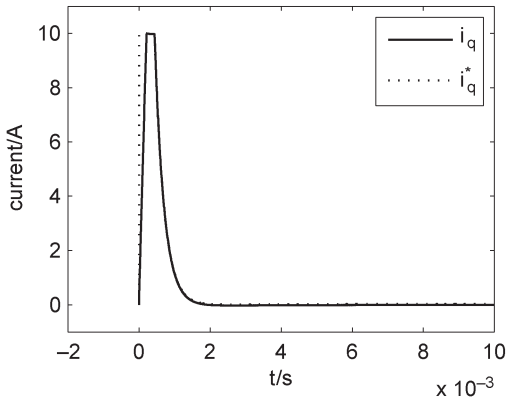

(b)

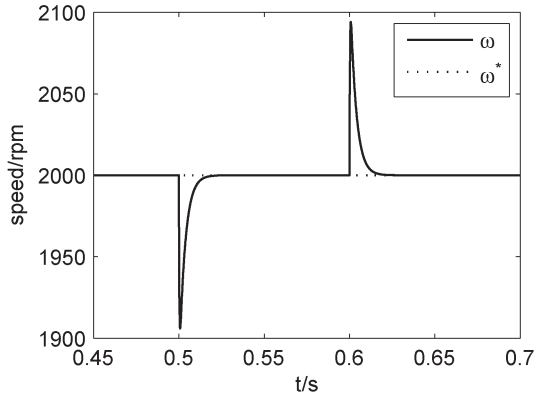

(c)

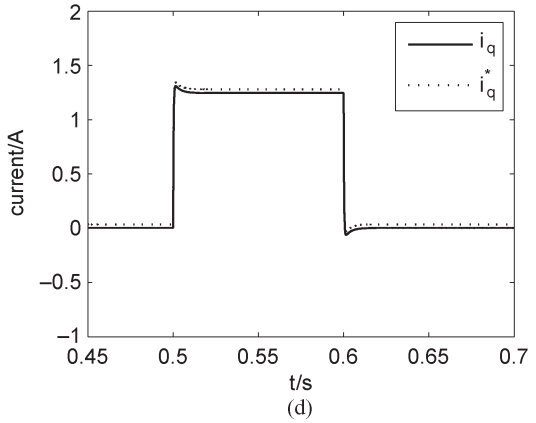

(d)

Fig. 5. Simulation responses under PI controller. (a) Speed. (b) i_q. (c) Speed in the case of load disturbance. (d) i_q in the case of load disturbance.

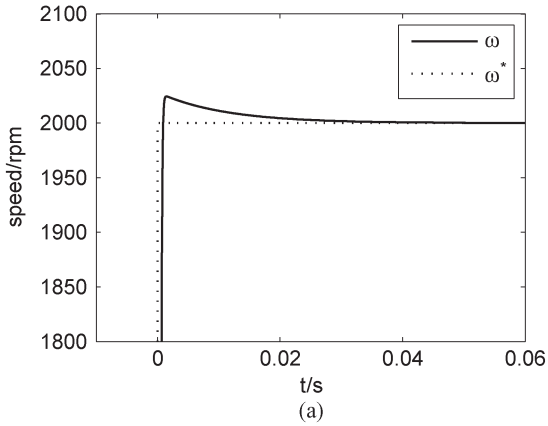

(a)

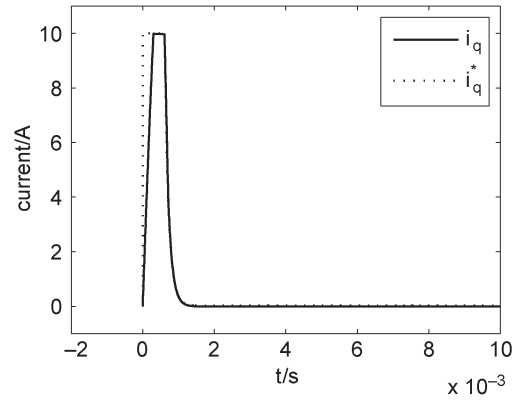

(b)

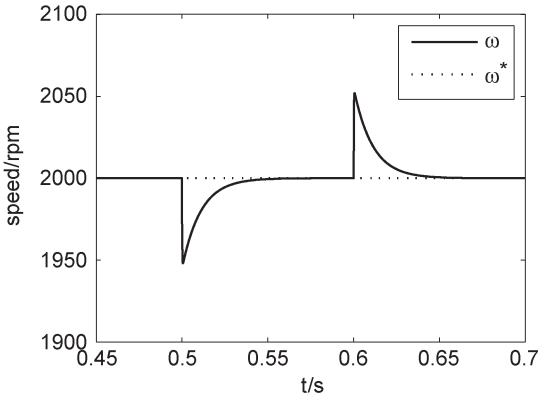

(c)

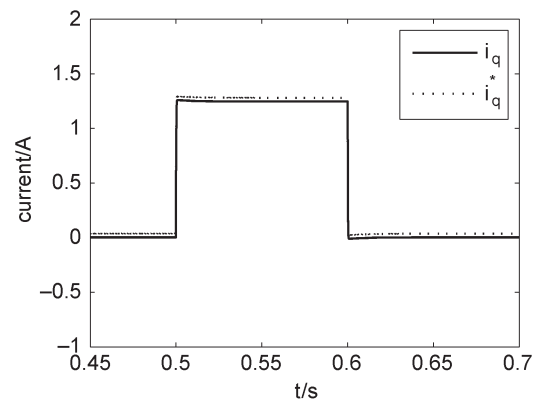

(d)

Fig. 6. Simulation responses under PFC controller. (a) Speed. (b) i_q. (c) Speed in the case of load disturbance. (d) i_q in the case of load disturbance.

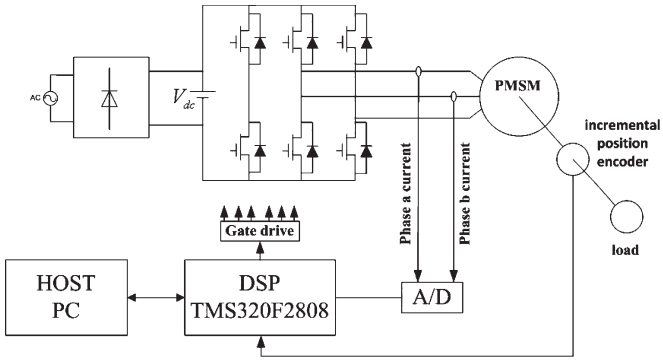

Fig. 7. Configuration of the experimental system.

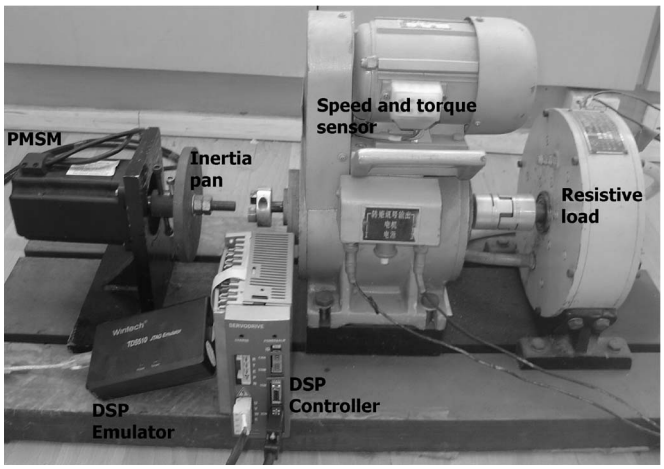

Fig. 8. Experimental test setup.

The control gains of both current loops are selected to be $K_p = 42$ and $K_i = 2600$. For the speed-loop control, parameters are chosen as: PI controller: $K_p = 0.02$, $K_i = 29$. PFC: $T_r = 50\ \mu$s, $P = 7$, $Q = I_{7\times 7}$, $r = 3.8$, $\alpha_m = 0.998$.

In this subsection, some experimental results are illustrated to confirm the simulation results. Figs. 9 and 10 show that the motor speed quickly converges to the reference value shortly after startup in the case of 2000 rpm reference speed.

Tests have also been performed to evaluate the performances of the proposed control system under sudden load disturbance impact. When the motor is running at a steady state of 2000 rpm, the load torque $T_L = 2.5\ \mathrm{N}\cdot\mathrm{m}$ is added suddenly and removed suddenly after some duration.

It can be observed that compared with the PI method, the PFC method shows a better disturbance rejection ability, with less speed fluctuations and shorter recovering times against disturbances.

D. Design Based on Predictive Functional Control and Extended State Observer

In order to improve the disturbance rejection performance of the PFC control method, a feedforward compensation part for the disturbances is introduced to the speed controller besides a PFC feedback part.

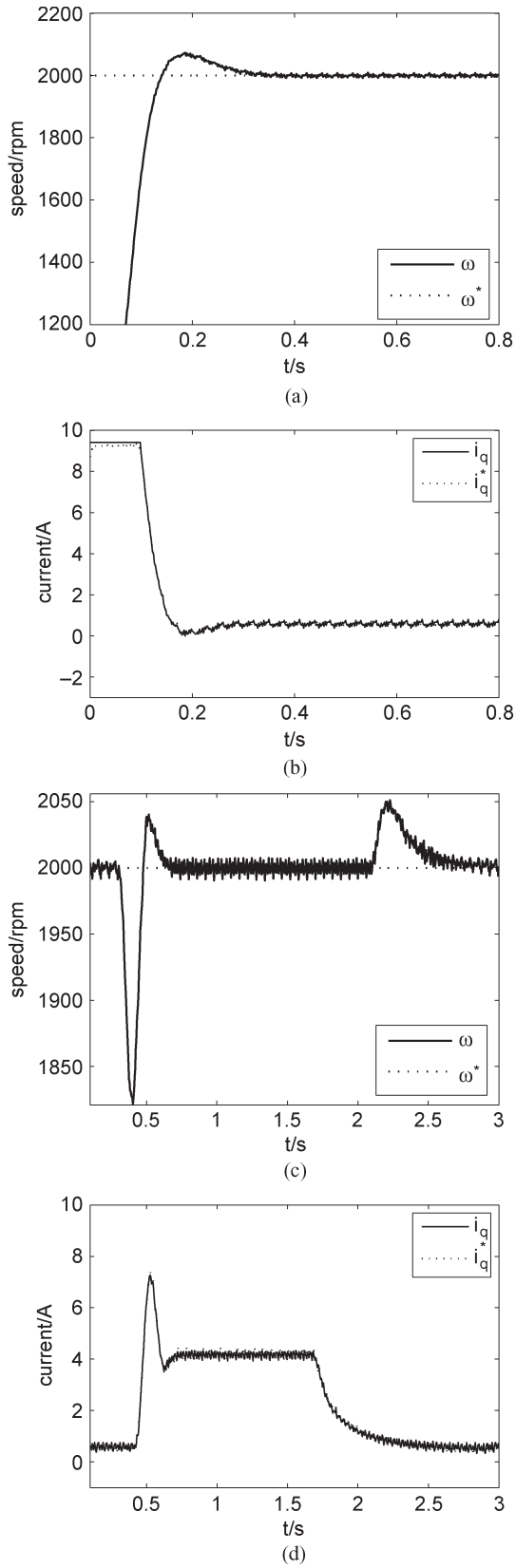

Fig. 9. Experimental responses under PI controller. (a) Speed. (b) i_q. (c) Speed in the case of load disturbance. (d) i_q in the case of load disturbance.

In this section, we consider a corresponding feedforward control design to compensate the disturbances. ESO is introduced as a kind of disturbance estimation technique for the

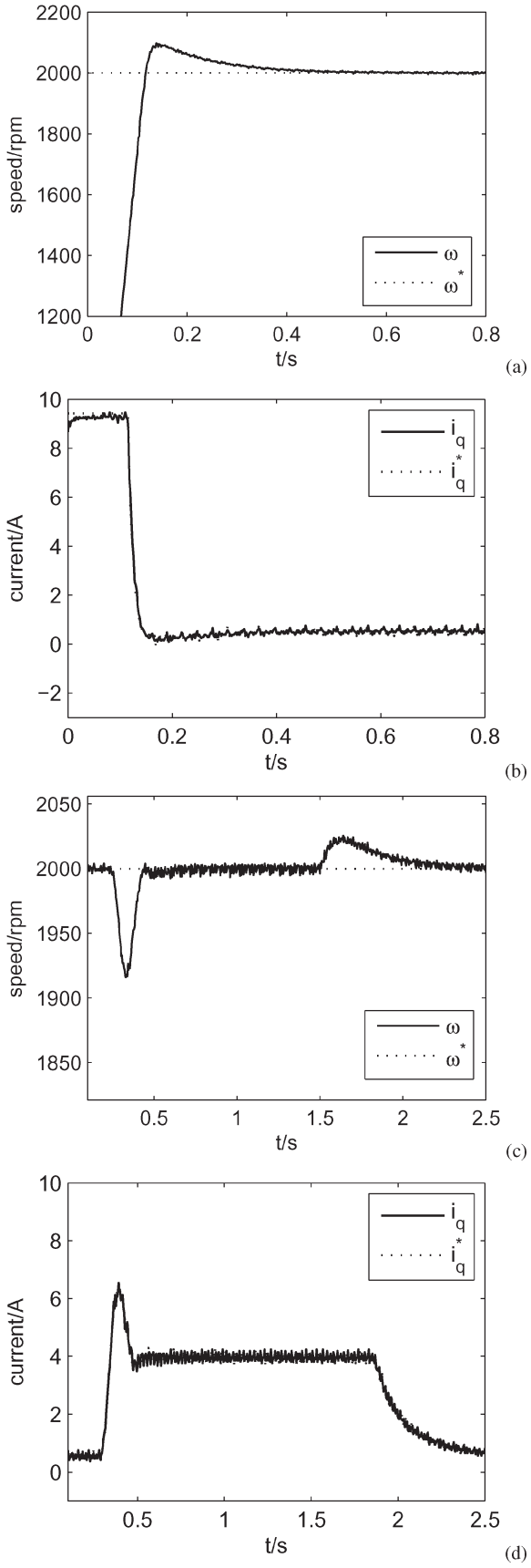

Fig. 10. Experimental responses under PFC controller. (a) Speed. (b) i_q. (c) Speed in the case of load disturbance. (d) i_q in the case of load disturbance.

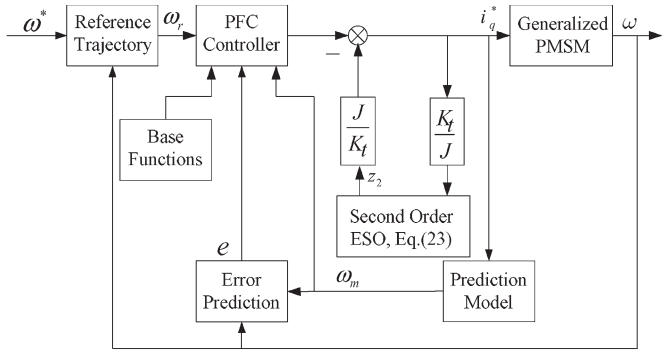

Fig. 11. Schematic diagram of the PMSM servo system under PFC+ESO.

PMSM servo system. The detail principle of ESO can be found in [28], [29]. Analysis of the performance of a second-order ESO and its applications can be found in [11], [32], [34].

The output of the system is the measured speed ω, and the motor dynamic equation from (1) can be rewritten as

$$\begin{aligned}\dot{\omega} &= \frac{K_t}{J}i_q - \frac{B}{J}\omega - \frac{T_L}{J} \\ &= \frac{K_t}{J}i_q^* - \frac{B}{J}\omega - \frac{T_L}{J} - \frac{K_t}{J}\left(i_q^* - i_q\right) \\ &= \frac{K_t}{J}i_q^* + d(t) \end{aligned} \tag{21}$$

where $d(t) = -(B\omega/J) - (T_L/J) - (K_t/J)(i_q^* - i_q)$ can be considered as the lumped disturbances including the friction, the external load disturbances, the tracking error of q-axis current loop.

Furthermore, we define $x_2 = d(t)$, $x_1 = \omega$, then (21) can be rewritten as the following state equation:

$$\begin{aligned}\dot{x}_1 &= x_2 + \frac{K_t}{J}i_q^* \\ \dot{x}_2 &= c(t) \end{aligned} \tag{22}$$

where $c(t)$ is the variation rate of system uncertainty and disturbance $d(t)$.

Then, a second-order linear ESO can be constructed for system (22) as follows:

$$\begin{cases} \dot{z}_1 = z_2 - 2p(z_1 - x_1) + b_0 i_q^* \\ \dot{z}_2 = -p^2(z_1 - x_1) \end{cases} \tag{23}$$

where $-p$ is the desired double pole of ESO with $p > 0$, b_0 is an estimate of K_t/J, z_1 is an estimate of speed ω, and z_2 is an estimate of the lumped disturbances $d(t)$. According to the analysis in [11], $z_1(t) \to \omega(t)$ and $z_2(t) \to a(t)$. Based on this information, compensation of disturbances can be achieved.

The control input of the composite controller is

$$\begin{aligned} i_q^*(k) = &\left(W_b^T Q W_b + R\right)^{-1} W_b^T Q \\ &\times \left[W_r(k) - W_o(k) - E(k)\right] - \frac{z_2(k)}{b_0}. \end{aligned} \tag{24}$$

This composite controller is composed of a feedforward part based-ESO and a feedback part based on PFC. With the

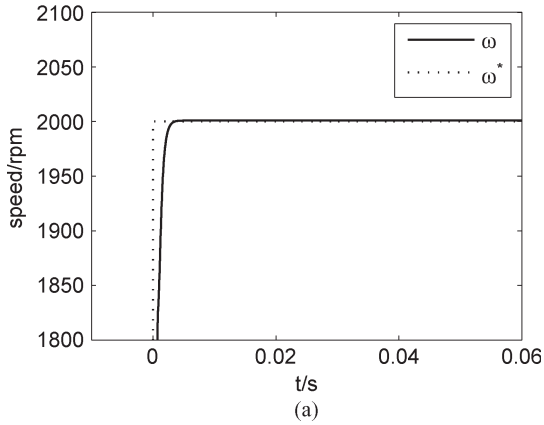

(a)

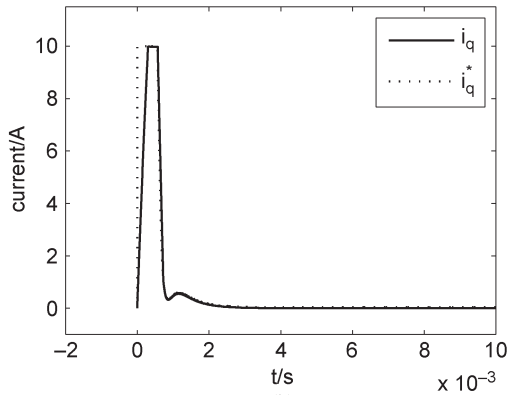

(b)

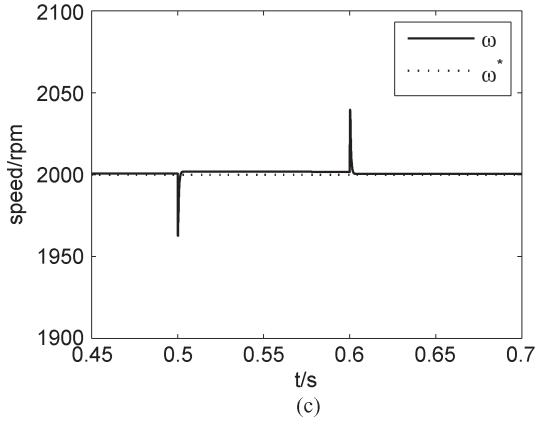

(c)

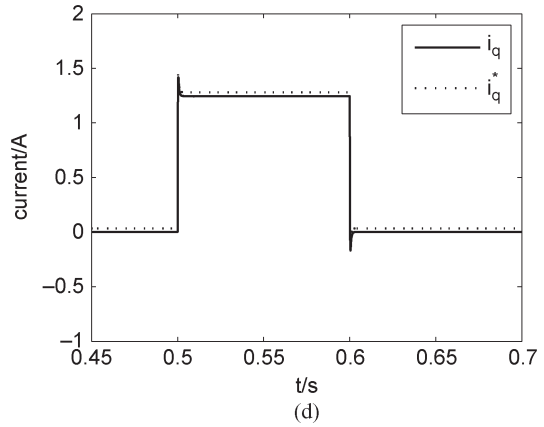

(d)

Fig. 12. Simulation responses under PFC+ESO controller. (a) Speed. (b) i_q. (c) Speed in the case of load disturbance. (d) i_q in the case of load disturbance.

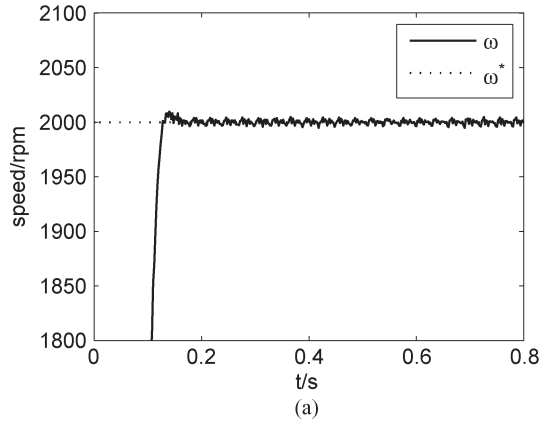

(a)

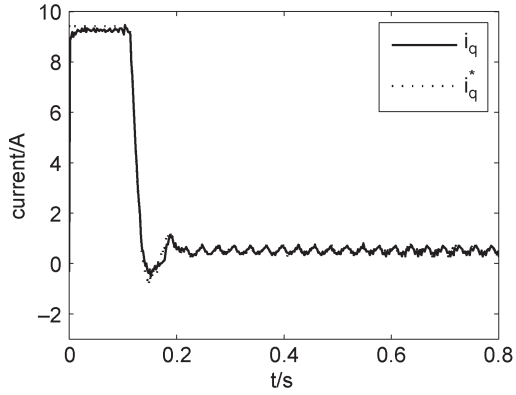

(b)

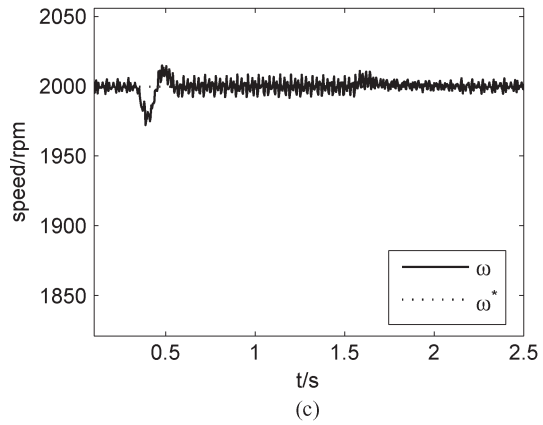

(c)

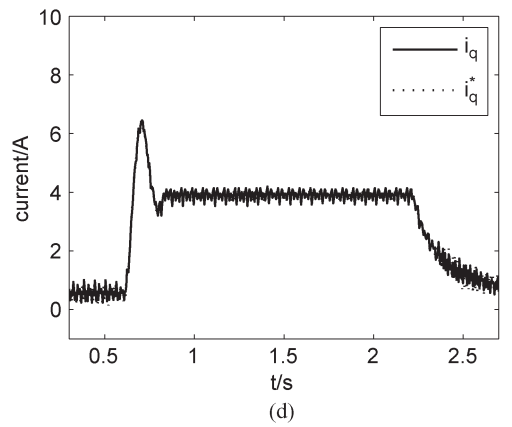

(d)

Fig. 13. Experimental speed responses under PFC+ESO controller. (a) Speed. (b) i_q. (c) Speed in the case of load disturbance. (d) i_q in the case of load disturbance.

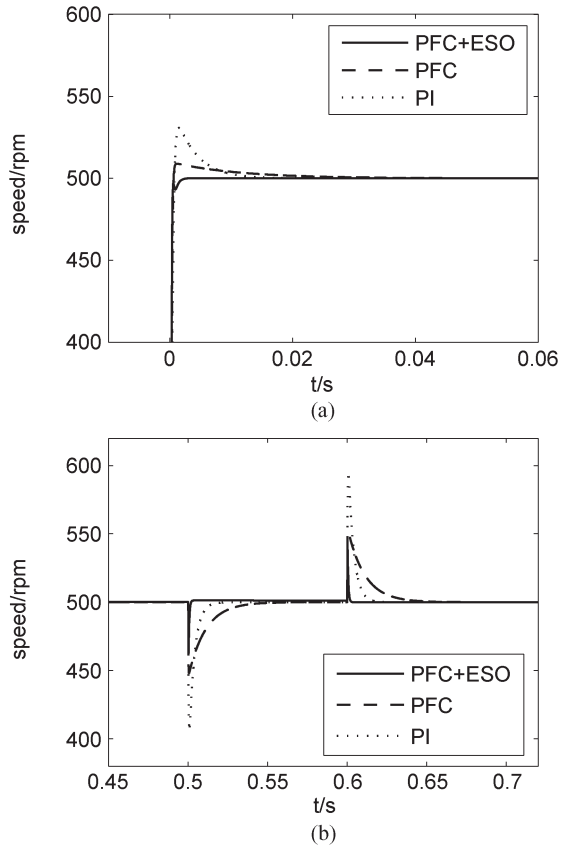

Fig. 14. Simulation responses under the three controllers in the case of 500 rpm reference speed. (a) Speed. (b) Speed in the case of load disturbance.

help of ESO, the system uncertainties and disturbances can be estimated and compensated instantaneously. This does good for the feedback control to improve the regulation ability. The schematic diagram of the composite PFC+ESO controller can be simplified as shown in Fig. 11.

E. Simulation and Experimental Results (PFC+ESO)

To demonstrate the efficiency of the proposed PFC+ESO method, simulations and experiments on a PMSM servo system have been performed. Here, some important indices, such as overshoot, settling time, fluctuation value, and integral of absolute error (IAE), are introduced to quantify the performance. IAE, which is the smaller the better, indicates the tracking performance of the system. It is defined as

$$IAE = \sum_{j=0}^{k} |\omega^*(j) - \omega(j)| . \tag{25}$$

1) Simulation Results: The parameters for PFC+ESO speed controller are: $-p = -4000$, $b_0 = 5414$, $T_s = 250$ μs, $T_r = 50$ μs, $P = 3$, $Q = I_{3\times 3}$, $r = 1.8$, $\alpha_m = 0.999$. The PI parameters of both current loops are the same as the other two kind of controllers.

Fig. 12 shows that compared with the PI and PFC methods, the PFC+ESO method has the shortest setting time and smallest overshoot. It can also be seen that, when a load torque $T_L = 2$ N $\cdot$ m is applied at $t = 0.5$ s and removed at $t = 0.6$ s, the

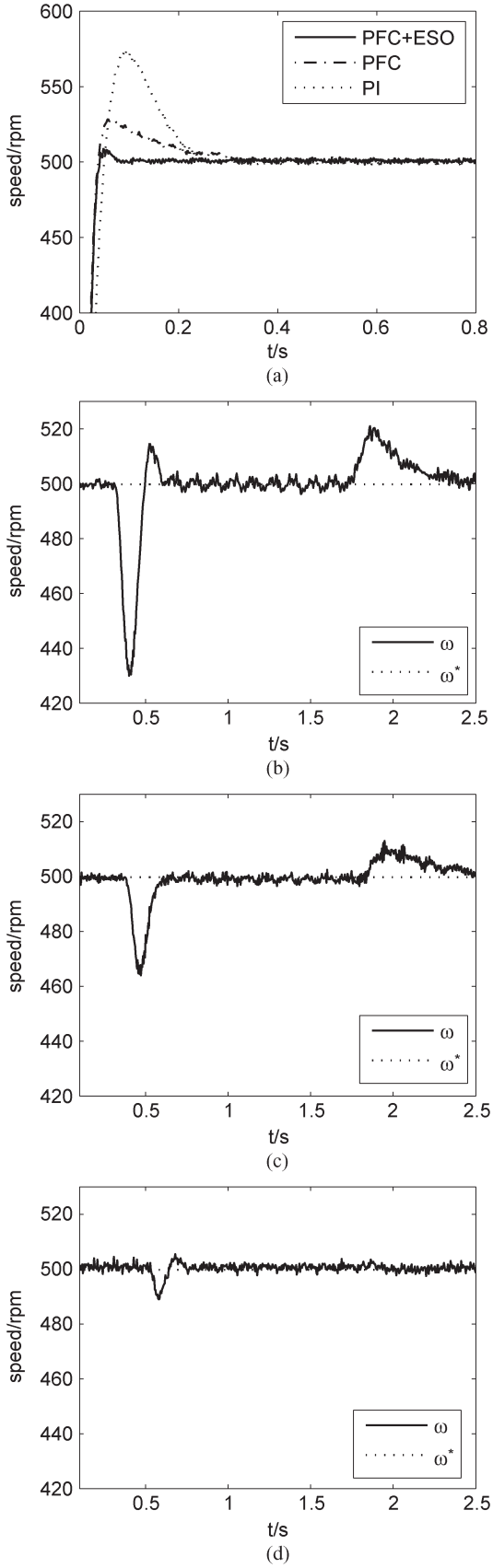

Fig. 15. Experimental responses under the three controllers in the case of 500 rpm reference speed. (a) Speed. (b) Speed in the case of load disturbance under PI controller. (c) Speed in the case of load disturbance under PFC controller. (d) Speed in the case of load disturbance under PFC+ESO controller.

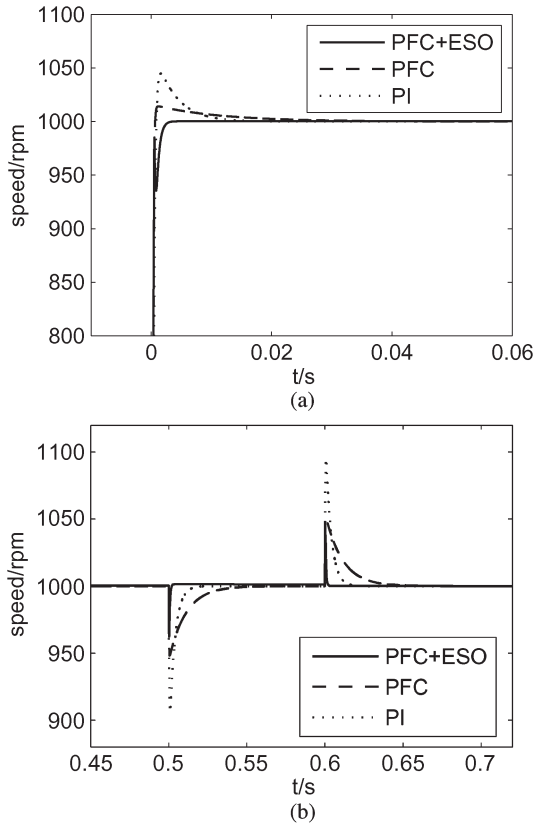

Fig. 16. Simulation responses under the three controllers in the case of 1000 rpm reference speed. (a) Speed. (b) Speed in the presence of load disturbance.

PFC+ESO-based controller has a shortest recovering time and smallest fluctuations.

2) Experimental Results: For the PFC+ESO speed controller, parameters are chosen as: $-p = -200$, $b_0 = 1274$, $T_r = 50\ \mu$s, $P = 5$, $Q = I_{5\times5}$, $r = 2.8$, $\alpha_m = 0.9995$. Fig. 13 shows that the motor speed quickly converges to the reference shortly after startup when the reference speed is given as 2000 rpm. Compared with other two controllers, the PFC+ESO method shows a smallest overshoot and a shortest settling time.

Tests have also been done to evaluate the performances of the proposed control system under sudden load disturbance impact. When the motor is running at a steady state of 2000 rpm, the load torque $T_L = 2.5\ \text{N}\cdot\text{m}$ is added suddenly and removed suddenly after some duration. The proposed PFC+ESO-based controller has a good disturbance rejection property while maintaining a good dynamic performance.

Considering the robustness of the PMSM servo system lastly, the comparison experiment results are also shown in Figs. 14–17 when the reference speed signals are given as 1000 rpm and 500 rpm, respectively. The parameters of three controllers at different operation conditions are still the same as that of the 2000 rpm case.

A comparison of performance indices on the three methods at different conditions are shown in Tables I–III. Please note that the tolerance band of settling time in this paper is selected as $\pm 2\%$. It can be observed that in all these three different work conditions, the PFC method has a better performance than the PI method and the PFC+ESO method has an overwhelming

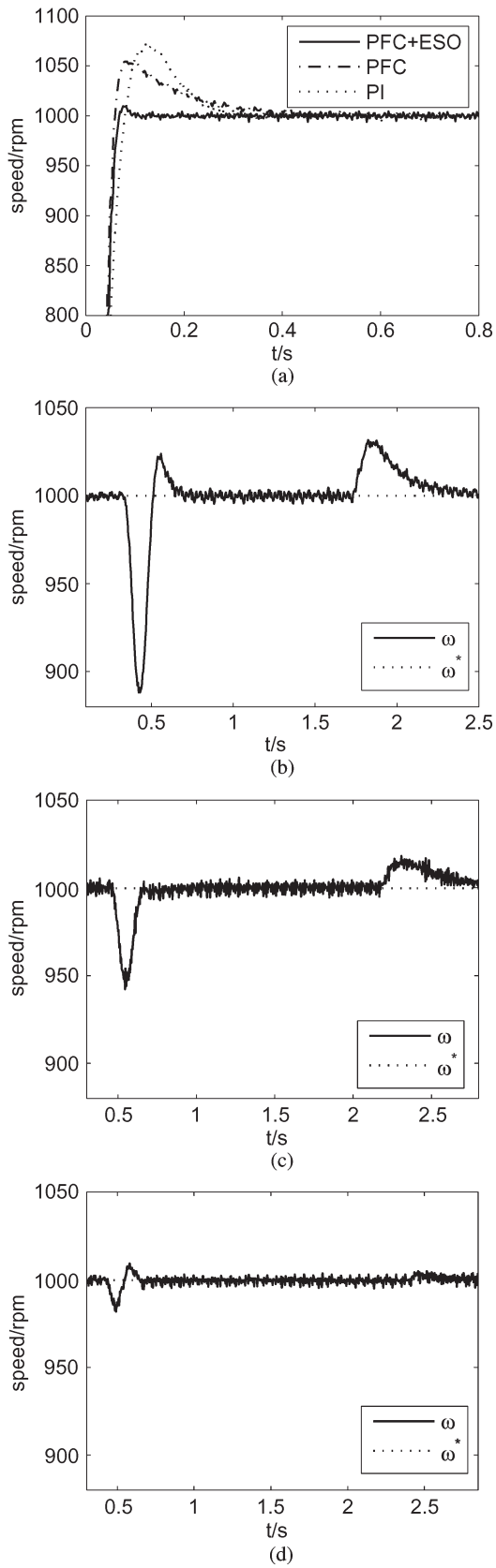

Fig. 17. Experimental responses under the three controllers in the case of 1000 rpm reference speed. (a) Speed. (b) Speed in the case of load disturbance under PI controller. (c) Speed in the case of load disturbance under PFC controller. (d) Speed in the case of load disturbance under PFC+ESO controller.

TABLE I
COMPARISON OF PERFORMANCE INDICES (2000 rpm)

Control Scheme		OS (%)	$t_s(ms)$	Speed Fluctuation/(rpm)	
				Increase	Decrease
Simulation	PI	2.08	2.2	94	94
	PFC	1.22	0.9	52	52
	PFC+ESO	0.05	2.0	40	40
Experiment	PI	3.65	244	51	178
	PFC	4.89	247	26	84
	PFC+ESO	0.50	121	12	33

TABLE II
COMPARISON OF PERFORMANCE INDICES (1000 rpm)

Control Scheme		OS (%)	$t_s(ms)$	Speed Fluctuation/(rpm)	
				Increase	Decrease
Simulation	PI	4.49	4.5	94	94
	PFC	1.43	0.8	52	52
	PFC+ESO	0.05	0.6	39	39
Experiment	PI	7.15	220	31	111
	PFC	5.45	207	18	58
	PFC+ESO	0.98	65	5	18

TABLE III
COMPARISON OF PERFORMANCE INDICES (500 rpm)

Control Scheme		OS (%)	$t_s(ms)$	Speed Fluctuation/(rpm)	
				Increase	Decrease
Simulation	PI	6.16	5.6	94	94
	PFC	1.79	0.6	52	52
	PFC+ESO	0.04	0.5	39	39
Experiment	PI	14.70	210	21	70
	PFC	5.70	193	13	36
	PFC+ESO	1.80	72	4	11

advantage on disturbance rejection. Also, from Fig. 18, we can see that both the PFC and PFC+ESO-based control systems have a smaller IAE at different conditions.

IV. CONCLUSION

In this paper, the design and implementation of a speed controller based on PFC for the PMSM system has been investigated. The simulation and experiment results show that the closed-loop systems under the proposed PFC method has achieved a satisfying dynamic performance. To further improve the disturbance rejection ability of the closed-loop system, a composite PFC control scheme which combines PFC and ESO

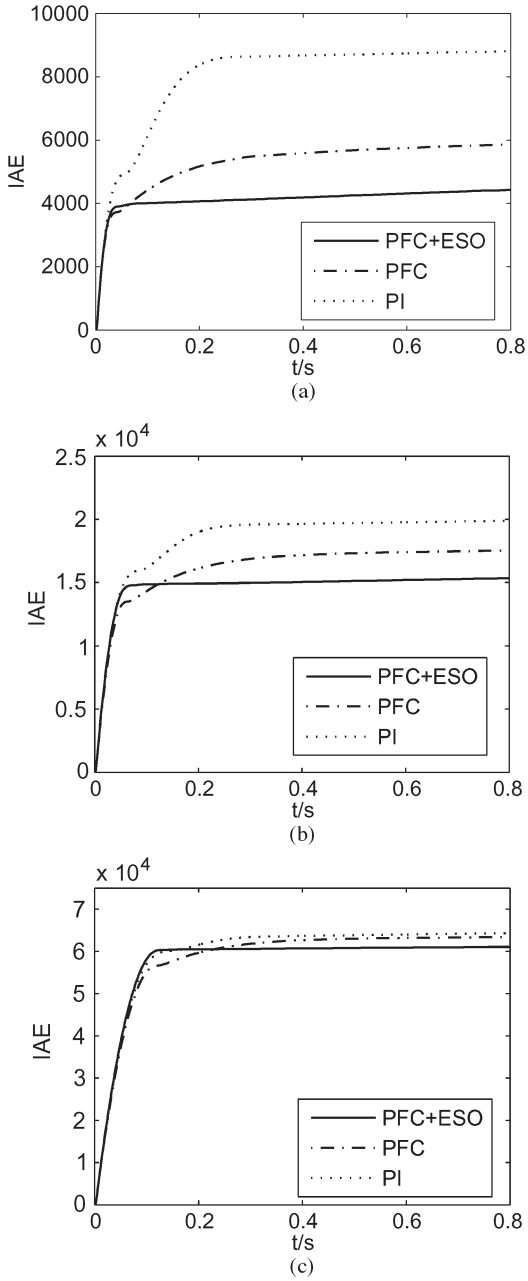

Fig. 18. Comparison of integral of absolute error (IAE) in different reference speed cases. (a) 500 rpm. (b) 1000 rpm. (c) 2000 rpm.

together has been developed. The simulation and experimental results have validated that the servo system under the composite PFC method can obtain a satisfying performance with fast transient response, good disturbances rejection ability.

REFERENCES

[1] R. Krishnan, *Electric Motor Drives: Modeling, Analysis, and Control*. Upper Saddle River, NJ, Unite States: Prentice-Hall, 2001.
[2] A. V. Sant and K. R. Rajagopal, "PM synchronous motor speed control using hybrid fuzzy-PI," *IEEE Trans. Magn.*, vol. 45, no. 10, pp. 4672–4675, Oct. 2009.
[3] G. J. Wang, C. T. Fong, and K. J. Chang, "Neural-network-based self-tuning PI controller for precise motion control of PMAC motors," *IEEE Trans. Ind. Electron.*, vol. 48, no. 2, pp. 408–415, Apr. 2001.
[4] H. A. Zarchi, G. R. A. Markadeh, and J. Soltani, "Direct torque and flux regulation of synchronous reluctance motor drives based on input-output

feedback linearization," *Energy Convers. Manag.*, vol. 51, no. 1, pp. 71–80, Jan. 2010.
[5] R. L. A. Ribeiro, A. D. Araujo, A. C. Oliveria, and C. B. Jacobina, "A high performance permanent magnet synchronous motor drive by using a robust adaptive control strategy," in *Proc. Power Electron. Spec. Conf.*, Orlando, FL, Jun. 2007, pp. 2260–2266.
[6] S. H. Li and Z. G. Liu, "Adaptive speed control for permanent-magnet synchronous motor system with variations of load inertia," *IEEE Trans. Ind. Electron.*, vol. 56, no. 8, pp. 3050–3059, Aug. 2009.
[7] F. J. Lin, T. S. Lee, and C. H. Lin, "Robust H_∞ controller design with recurrent neural network for linear synchronous motor drive," *IEEE Trans. Ind. Electron.*, vol. 50, no. 3, pp. 456–470, Jun. 2003.
[8] F. F. M. El-Sousy, "Hybrid H-infinity-based wavelet-neural-network tracking control for permanent-magnet synchronous motor servo drives," *IEEE Trans. Ind. Electron.*, vol. 57, no. 9, pp. 3157–3166, Sep. 2010.
[9] C. K. Lai and K. K. Shyu, "A novel motor drive design for incremental motion system via sliding-mode control method," *IEEE Trans. Ind. Electron.*, vol. 52, no. 2, pp. 499–507, Apr. 2005.
[10] I. C. Baik, K. H. Kim, and M. J. Youn, "Robust nonlinear speed control of PM synchronous motor using boundary layer integral sliding mode control technique," *IEEE Trans. Control Syst. Technol.*, vol. 8, no. 1, pp. 47–54, Jan. 2000.
[11] R. Miklosovic and Z. Q. Gao, "A robust two-degree-of-freedom control design technique and its practical application," in *Conf. Rec. 39th IEEE IAS Annu. Meeting*, Oct. 3–7, 2004, vol. 3, pp. 1495–1502.
[12] S. H. Li, H. X. Liu, and S. H. Ding, "A speed control for a PMSM using finite-time feedback control and disturbance compensation," *Trans. Inst. Meas. Control*, vol. 32, no. 2, pp. 170–187, Apr. 2010.
[13] K. H. Kim and M. J. Youn, "A nonlinear speed control for a PM synchronous motor using a simple disturbance estimation technique," *IEEE Trans. Ind. Electron.*, vol. 49, no. 3, pp. 524–535, Jun. 2002.
[14] Y. Luo, Y. Q. Chen, H.-S. Ahnc, and Y. G. Pi, "Fractional order robust control for cogging effect compensation in PMSM position servo systems: Stability analysis and experiments," *Control Eng. Pract.*, vol. 18, no. 9, pp. 1022–1036, Sep. 2010.
[15] R. J. Wai, "Hybrid fuzzy neural-network control for nonlinear motor-toggle servomechanism," *IEEE Trans. Control Syst. Technol.*, vol. 10, no. 4, pp. 519–532, Jul. 2002.
[16] J. M. Maciejowski, *Predictive Control With Constraints*. London, U.K.: Prentice-Hall, Jun. 2001.
[17] W. H. Chen, D. J. Ballance, and P. J. Gawthrop, "Optimal control of nonlinear systems: A predictive control approach," *Automatica*, vol. 39, no. 4, pp. 633–641, Apr. 2003.
[18] C. Line, C. Manzie, and M. C. Good, "Electromechanical brake modeling and control: From PI to MPC," *IEEE Trans. Control Syst. Technol.*, vol. 16, no. 3, pp. 446–457, May 2008.
[19] F. Morel, X. F. Lin-Shi, J. M. Retif, B. Allard, and C. Buttay, "A comparative study of predictive current control schemes for a permanent-magnet synchronous machine drive," *IEEE Trans. Ind. Electron.*, vol. 56, no. 7, pp. 2715–2728, Jul. 2009.
[20] S. Matsutani, T. Zanma, Y. Sumiyoshi, M. Ishida, A. Imura, and M. Fujitsuna, "Optimal control of PMSMs using model predictive control with integrator," in *Proc. ICCAS-SICE*, Aug. 2009, vol. 10–13, pp. 4847–4852.
[21] S. Bolognani, S. Bolognani, L. Peretti, and M. Zigliotto, "Design and implementation of model predictive control for electrical motor drives," *IEEE Trans. Ind. Electron.*, vol. 56, no. 6, pp. 1925–1936, Jun. 2009.
[22] J. Richalet, "Industrial applications of model based predictive control," *Automatica*, vol. 29, no. 5, pp. 1251–1274, Sep. 1993.
[23] H. B. Kuntze, A. Jacubasch, U. Hirsch, J. Richalet, and C. Arber, "On the application of a new method for fast and robust position control of industrial robots," in *Proc. IEEE Int. Conf. Robot. Autom.*, Apr. 1988, vol. 3, pp. 1574–1580.
[24] T. F. H. C. Ernst, "First principle modeling and predictive functional control of enthalpic processes," Ph.D. dissertation, Delft Univ. Technol., Delft, The Netherlands, 1996.
[25] R. D. Zhang and S. Q. Wang, "Predictive functional controller with a similar proportional integral optimal regulator structure: Comparison with traditional predictive functional controller and application to heavy oil cooking equipment," *Chin. J. Chem. Eng.*, vol. 15, no. 2, pp. 247–253, Mar. 2007.
[26] M. Lepeti, I. Skrjanc, H. G. Chiacchiarini, and D. Matko, "Predictive functional control based on fuzzy model: Magnetic suspension system case study," *Eng. Appl. Artif. Intell.*, vol. 16, no. 5/6, pp. 425–430, Aug./Sep. 2003.
[27] D. Dejan and I. Skrjanc, "Predictive functional control based on an adaptive fuzzy model of a hybrid semi-batch reactor," *Control Eng. Pract.*, vol. 18, no. 8, pp. 979–989, Aug. 2010.
[28] J. Q. Han, "The extended states observer of a class of uncertain systems," (in Chinese), *Control Decis.*, vol. 10, no. 1, pp. 85–88, 1995.
[29] J. Q. Han, "From PID to active disturbance rejection control," *IEEE Trans. Ind. Electron.*, vol. 56, no. 3, pp. 900–906, Mar. 2009.
[30] J. Su, W. Qiu, H. Ma, and P.-Y. Woo, "Calibration-free robotic eye-hand coordination based on an auto disturbance-rejection controller," *IEEE Trans. Robot.*, vol. 20, no. 5, pp. 899–907, Oct. 2004.
[31] D. Wu, K. Chen, and X. Wang, "Tracking control and active disturbance rejection with application to noncircular machining," *Int. J. Mach. Tools Manuf.*, vol. 47, no. 15, pp. 2207–2217, Dec. 2007.
[32] Y. X. Su, B. Y. Duan, C. H. Zheng, Y. F. Zhang, G. D. Chen, and J. W. Mi, "Disturbance-rejection high-precision motion control of a Stewart platform," *IEEE Trans. Control Syst. Technol.*, vol. 12, no. 3, pp. 364–374, May 2004.
[33] B. Sun and Z. Gao, "A DSP-based active disturbance rejection control design for a 1-kW H-bridge dc–dc power converter," *IEEE Trans. Ind. Electron.*, vol. 52, no. 5, pp. 1271–1277, Oct. 2005.
[34] Y. X. Su, C. H. Zheng, and B. Y. Duan, "Automatic disturbances rejection controller for precise motion control of permanent-magnet synchronous motors," *IEEE Trans. Ind. Electron.*, vol. 52, no. 3, pp. 814–823, Jun. 2005.
[35] G. Feng, L. P. Huang, and D. Q. Zhu, "A new robust algorithm to improve the dynamic performance on the speed control of induction motor drive," *IEEE Trans. Power Electron.*, vol. 19, no. 6, pp. 1614–1627, Nov. 2004.
[36] J. F. Pan, N. C. Cheung, and J. M. Yang, "Auto-disturbance rejection controller for novel planar switched reluctance motor," *Proc. Inst. Elect. Eng.—Elect. Power Appl.*, vol. 153, no. 2, pp. 307–315, Mar. 2006.
[37] D. Sun, "Comments on active disturbance rejection control," *IEEE Trans. Ind. Electron.*, vol. 54, no. 6, pp. 3428–3429, Dec. 2007.
[38] Y. Xia, P. Shi, G.-P. Liu, and D. Rees, "Active disturbance rejection control for uncertain multivariable systems with time-delay," *IET Control Theory Appl.*, vol. 1, no. 1, pp. 75–81, Jan. 2007.
[39] A. S. Hodel, "Variable-structure PID control to prevent integrator windup," *IEEE Trans. Ind. Electron.*, vol. 48, no. 2, pp. 442–451, Jan. 2001.

Huixian Liu was born in Ninjin, China, in 1984. She received the B.S. degree in automation from Hebei University of Science and Technology, Shijiazhuang, China, in 2006. She is now working toward the Ph.D. degree from the School of Automation, Southeast University, Nanjing.

Her research interests include nonlinear system control, predictive control with applications to AC motors.

Shihua Li (M'05–SM'10) was born in Pingxiang, China, in 1975. He received the Bachelor, Master, and Ph.D. degrees all in automatic control from Southeast University, Nanjing, China, in 1995, 1998, and 2001, respectively.

Since 2001, he has been with School of Automation, Southeast University, where he is currently a professor. His main research interests include nonlinear control theory with applications to robots, spacecraft, ac motors, and other mechanical systems.